



Comparative Thermogravimetric and Differential Thermal Analysis of Bio-synthesized MgO-Nanoparticles using *Chromolaena odorata*, *Hevea brasiliensis*, and *Elaeis guineensis* Leaf Extracts

*Godfrey Osatohanmwun OTABOR¹, Esther Uwidia IKHUORIA², Joshua Osaretin ONAIFO¹, Ikhazuagbe Hilary IFIJEN³, Aiyevbekpen Clinton EHIGIE², Aireguamen I. AIGBODION⁴

¹Department of Chemistry, Faculty of Physical Sciences, Ambrose Alli University, Ekpoma, Edo State, Nigeria

²Department of Chemistry, Faculty of Physical Sciences, University of Benin, P.M.B. 1154, Benin City, Edo State, Nigeria

³Department of Research Outreach, Rubber Research Institute of Nigeria, Iyanomo, P.M.B, 1049, Benin City, Edo State, Nigeria

⁴Department of Physical Sciences (Chemistry Option), Benson Idahosa University, Benin City, Edo State, Nigeria

*Correspondence Email: godfreyotabor@aauekpoma.edu.ng

Article information

Article history: Received December 2024

Revised December 2024

Accepted December 2024

Published online January 2025

Copyright: © 2025 Otabor *et al.* This open-access article is distributed under the terms of the Creative Commons Attribution License, which permits unrestricted use, distribution, and reproduction in any medium, provided the original author and source are credited.

ABSTRACT

Magnesium oxide (MgO) nanoparticles are highly versatile, finding applications in catalysis, antibacterial treatments, and refractory materials. This study explores the eco-friendly biosynthesis of MgO nanoparticles using leaf extracts from *Hevea brasiliensis* (Rubber tree), *Chromolaena odorata* (Awolowo plant), and *Elaeis guineensis* (Oil Palm), capitalizing on their phytochemical richness. Thermogravimetric Analysis (TGA) revealed distinct thermal degradation patterns. *H. brasiliensis*-mediated nanoparticles exhibited multi-step weight loss, with a residual content of 24.36%, while *E. guineensis*-based nanoparticles showed a two-phase degradation with a residue of 25.5%. *C. odorata*-derived nanoparticles demonstrated the highest thermal stability, with a single extended phase and 28.9% residue. Differential Thermal Analysis (DTA) highlighted energy release variations, with *C. odorata*-mediated nanoparticles displaying the most thermally stable exothermic peaks. These results emphasize the influence of plant extracts on the thermal properties of MgO nanoparticles and highlight biosynthesis as a sustainable method for producing thermally tailored nanoparticles for specialized applications.

Keywords: Awolowo, Green-synthesis, Oil-palm, Rubber and Leaf Extracts,

1.0 INTRODUCTION

Nanoparticles are a versatile and indispensable class of materials, playing significant roles across diverse sectors, including manufacturing, medicine, and energy. Their unique properties have fueled advancements in product development and technological applications [1]. The primary classes of nanoparticles integrated into these innovations include carbon-based materials (such as nanotubes and fullerenes), metallic nanoparticles (gold, silver, iron, and copper), metal oxides (e.g., MgO, ZnO, TiO₂, CeO₂, SiO₂), and quantum dots [2]. Among these, magnesium oxide (MgO) nanoparticles have garnered attention for their applications in catalysis, antibacterial treatments, and as additives in refractory materials [3]. Despite their potential, traditional

synthesis methods for MgO nanoparticles often involve toxic chemicals and energy-intensive processes. This has prompted a shift toward greener and more sustainable synthesis approaches, such as biosynthesis, which leverages natural resources to minimize environmental impact [4]. Biosynthesis of nanoparticles utilizes plant extracts rich in phytochemicals like flavonoids, alkaloids, and tannins, which act as reducing and stabilizing agents [5]. The characterization of bio-synthesized nanoparticles is essential for understanding their properties and potential applications. Common techniques include microscopy such as scanning electron microscopy (SEM) and transmission electron microscopy (TEM) provide insights into particle size, shape,

morphology, and crystallinity [11, 12], spectroscopy methods: including Raman spectroscopy, UV-Vis spectroscopy, and Fourier transform infrared (FTIR) spectroscopy, reveal details about electronic structures, surface chemistry, and functional groups [13, 14]; while elemental analysis like X-ray fluorescence spectroscopy, complement these analyses by providing detailed compositional data [15]. Particle sizing methods like dynamic light scattering (DLS) offers additional information on particle size and distribution [16]. including Raman spectroscopy, UV-Vis spectroscopy, and Fourier transform infrared (FTIR) spectroscopy, reveal details about electronic structures, surface chemistry, and functional groups [13, 14]; while elemental analysis like X-ray fluorescence spectroscopy, complement these analyses by providing detailed compositional data [15]. Particle sizing methods like dynamic light scattering (DLS) offers additional information on particle size and distribution [16]. Thermal methods of analysis, such as Thermogravimetric analysis (TGA) and Differential thermal analysis (DTA), are critical for assessing the thermal stability and composition of nanoparticles. These techniques provide rapid insights into decomposition patterns, exothermic and endothermic transitions, and overall thermal behavior [17, 18]. In particular, TGA quantifies weight losses during heating, helping to determine impurities and encapsulated materials within nanoparticles [19, 20].

This study focuses on the biosynthesis of MgO nanoparticles using the extracts of *Hevea brasiliensis* (Rubber tree), *Chromolaena odorata* (Awolowo plant), and *Elaeis guineensis* (Oil palm) and investigation of their thermal behaviour. These plants were selected for their abundance in tropical regions and their rich phytochemical profiles. The Rubber tree, renowned for latex production, also contains bioactive compounds in its leaves [6, 7]. Similarly, the Awolowo plant, known for its medicinal properties, is rich in secondary metabolites suitable for nanoparticle synthesis [8, 9]. Oil palm leaves, often regarded as agricultural waste, hold untapped potential due to

their valuable phytochemicals [10]. Through comprehensive TGA/DTA analysis, the study aims to elucidate the thermal stability, composition, and potential applications of these bio-synthesized nanoparticles. Furthermore, by contributing to the growing knowledge of green synthesis methods, this work seeks to advance the development of sustainable nanotechnologies for various scientific and industrial applications.

2.0 MATERIALS AND METHODS

Chemicals utilized in this study were magnesium nitrate hexahydrate ($Mg(NO_3)_2 \cdot 6H_2O$), sodium hydroxide were obtained from Sigma Aldrich and were used without further purification; double-distilled water and freshly collected Awolowo, Oil palm and rubber leaves.

2.1 Sample Preparation

The leaves were collected fresh as shown in plates 1, 2 and 3. They were properly washed with distilled water to remove any impurities such as sand and dust. The samples were then dried at room temperature to a constant weight. The dried leaves were blended into fine powder and stored in an airtight container for further use.

2.2 Preparation of leaves extracts

Ten grammes of each leaf sample were boiled in 200 mL distilled water in a 500 mL beaker individually and agitated at a temperature of 70°C for approximately 30 minutes. The resultant solution was initially filtrated using cotton wool before employing filter paper (Whatman No.1). The acquired extract was preserved in the refrigerator until needed.

2.3 Biosynthesis of MgO nanoparticles

The method described by Ikhuoria *et al* [21] was used in the green synthesis of magnesium oxide (MgO) nanoparticles using the different leaf extracts.

2.4 TGA/DTA CHARACTERIZATION OF MgO-NPs

The thermal stability of biosynthesized Magnesium Oxide nanoparticles (MgONPs), capped by phytochemicals from Oil Palm, Rubber, and Awolowo leaf aqueous extracts, was investigated using Thermogravimetric Analysis (TGA) and Differential Thermal Analysis (DTA). The experiments were conducted using a Shimadzu Q50 TGA thermal analyzer under a nitrogen atmosphere, with a heating rate of 20°C per minute. Nitrogen was chosen as the horizontal flow gas to prevent additional mass loss due to oxidation of the sample material [22].

3.0 RESULTS AND DISCUSSION Table 1: TGA/DTA results of Oil palm, Awolowo and Rubber leaf mediated MgONPs

| S/N | Temp. (°C) | TGA | DTA | TGA | DTA | TGA | DTA |
|-----|------------|---------------|---------|-------------|---------|--------------|---------|
| | | (%wt) | (°C/mg) | (%wt) | (°C/mg) | (%wt) | (°C/mg) |
| | | Oil palm leaf | | Rubber leaf | | Awolowo leaf | |
| 1 | 200 | 77.13 | 0.011 | 88.72 | 0.016 | 88.14 | 0.022 |
| 2 | 250 | 77.35 | 0.013 | 84.61 | 0.030 | 88.14 | 0.023 |
| 3 | 300 | 77.38 | 0.014 | 82.70 | 0.014 | 88.14 | 0.021 |
| 4 | 350 | 72.60 | 0.015 | 76.03 | 0.020 | 88.14 | 0.021 |
| 5 | 400 | 68.39 | 0.020 | 64.85 | 0.064 | 88.16 | 0.023 |
| 6 | 450 | 50.63 | 0.028 | 64.30 | 0.017 | 88.13 | 0.026 |
| 7 | 500 | 44.72 | 0.028 | 86.70 | 0.018 | 88.10 | 0.043 |
| 8 | 550 | 34.81 | 0.042 | 48.53 | 0.021 | 70.32 | 0.063 |
| 9 | 600 | 34.53 | 0.072 | 44.76 | 0.028 | 55.80 | 0.054 |
| 10 | 650 | 34.06 | 0.013 | 40.84 | 0.006 | 37.26 | 0.039 |
| 11 | 700 | 34.06 | 0.014 | 36.50 | 0.003 | 39.26 | 0.031 |
| 12 | 750 | 34.06 | 0.014 | 35.43 | 0.003 | 36.41 | 0.024 |
| 13 | 800 | 34.06 | 0.014 | 35.45 | 0.004 | 35.97 | 0.023 |
| 14 | 850 | 34.06 | 0.010 | 35.31 | 0.005 | 34.50 | 0.023 |

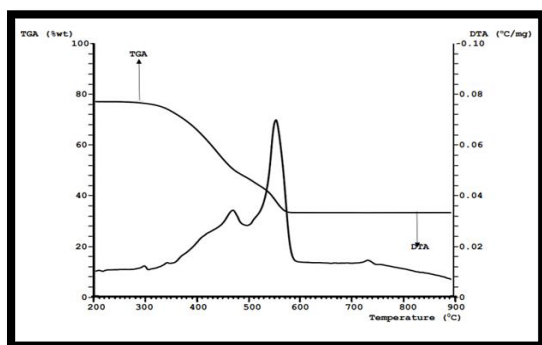


Figure 1: TGA/DTA spectra of Oil palm leaf (*Elaeis guineensis*) (MgONPs) sample

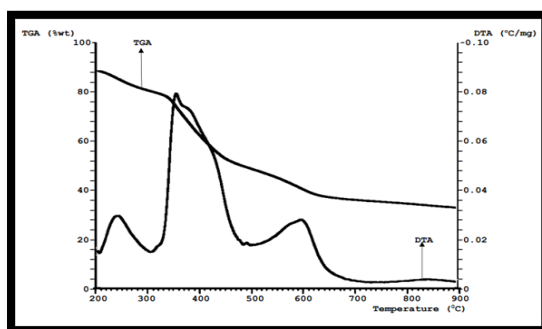


Figure 2: TGA/DTA spectra of Rubber leaf (*Hevea brasiliensis*) (MgO) sample

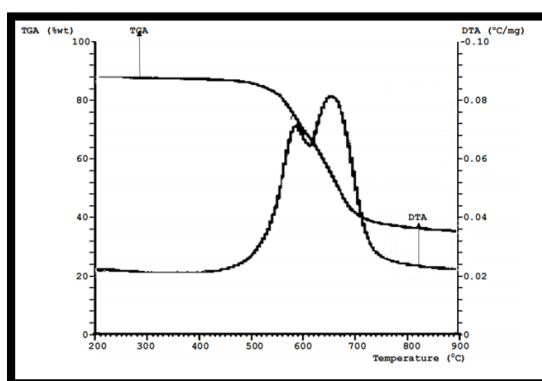


Figure 3: TGA/DTA Spectra of Awolowo leaf (*Chromolaena odorata*) MgONPs

Table 1 shows the TGA/DTA results of MgONPs mediated with the different leaf extracts. The degradation patterns observed reveal distinct behaviors, indicating variations in their thermal stability. These differences can be attributed to the unique composition of the phytochemicals present in each plant source. Rubber and Oil Palm leaf-derived MgO nanoparticles (Figures 1 and 2) exhibit multi-step degradation, a characteristic indicative of the layered nature of phytochemical decomposition. This multi-step degradation behavior is consistent with the findings of Venkatachalam et al. [23], who reported a similar phenomenon in MgO nanoparticles synthesized from *Moringa*. The multi-step degradation process suggests the sequential breakdown of different

phytochemicals, with each decomposing at distinct temperature ranges, contributing to a staggered thermal stability profile. In contrast, MgO nanoparticles synthesized from Awolowo leaves (Figure 3) show a single-step degradation pattern, which suggests a more uniform composition of phytochemicals that degrade more cohesively at higher temperatures. This behavior aligns with the TGA results observed by Mrig et al [24], who reported a continuous weight loss without distinct multi-step degradation phases.

The TGA analysis of rubber leaf-derived MgO nanoparticles (Figure 2) indicates a multi-step degradation process. Initially, a weight loss of 9.09% is observed between 220°C and 325°C, which is likely due to the evaporation of surface-adsorbed moisture and the volatilization of low-molecular-weight phytochemicals [25]. This initial phase suggests the removal of volatile components that are weakly adhered to the nanoparticle surfaces. Subsequently, a significant weight loss of 50% occurs between 330°C and 625°C, which corresponds to the decomposition and evaporation of stabilizing phytochemicals or biomolecules acting as capping agents on the nanoparticles [26]. The breakdown of these organic components accounts for the major weight loss in this phase. After the thermal degradation, the remaining residue is 24.36%, primarily consisting of stable inorganic MgO, which can withstand high temperatures without undergoing further decomposition. In comparison, MgO nanoparticles derived from Oil Palm leaves (Figure 1) display a different thermal degradation profile. The initial weight loss is more pronounced at 33.33%, occurring between 300°C and 460°C. This phase likely represents the decomposition of the first layer of phytochemicals and the removal of adsorbed water. A second weight loss of 34.61% is observed between 460°C and 575°C, indicating the breakdown of more complex and stable organic components. The residue remaining after thermal degradation is 25.5%, which is similar to that observed for rubber leaf-derived MgO nanoparticles, suggesting that both types contain a comparable proportion of stable inorganic MgO in the final product, despite the differences in degradation stages.

The thermal degradation behavior of MgO nanoparticles derived from Awolowo leaves (Figure 3) deviates significantly from the other two samples. Notably, no weight loss is observed between 200°C and 480°C, or between 790°C and 900°C, indicating the thermal stability of the nanoparticles within these temperature ranges. The primary degradation phase occurs as a single, extended phase between 480°C and 790°C, resulting in a continuous weight loss of approximately 59%. Unlike the multi-step degradation observed in rubber and Oil Palm leaf nanoparticles, the Awolowo leaf-derived MgO nanoparticles undergo a single, continuous degradation process. The residue after thermal

degradation is 28.9%, slightly higher than the residues for the other two samples. This higher residual content suggests a greater proportion of stable inorganic MgO, indicating that the nanoparticles from Awolowo leaves may contain more thermally stable components. Magnesium oxide (MgO) itself is a stable compound with a high melting point of approximately 2800°C, which does not undergo significant decomposition under typical TGA conditions (up to 900°C). Therefore, the weight loss observed in TGA studies of MgO nanoparticles is primarily attributed to the decomposition of the organic stabilizing agents, rather than the MgO core itself [27].

Differential thermal analysis (DTA) provides additional insights into the energy release associated with various physical and chemical transformations in the materials synthesized. The exothermic peaks observed in the DTA profiles of MgO nanoparticles synthesized from different leaf sources reveal distinct energy release patterns, which reflect the unique composition and interactions within each type of nanoparticle [28]. The MgO nanoparticles synthesized from rubber leaves exhibit exothermic peaks at 240°C, 360°C, and 600°C (Figure 2). These peaks indicate distinct stages of energy release associated with specific transformations within the nanoparticles. The exothermic peak at 240°C likely corresponds to the combustion or oxidative degradation of surface-adsorbed organic molecules and low-molecular-weight phytochemicals. The peak at 360°C suggests a further stage of energy release, possibly due to the breakdown of more stable organic components or capping agents on the nanoparticles' surfaces. The final exothermic peak at 600°C reflects the energy release from the decomposition of remaining complex organic molecules or the transformation of inorganic components within the nanoparticles [29]. In contrast, MgO nanoparticles derived from Oil Palm leaves (Figure 1) display exothermic peaks at 470°C and 560°C. The peak at 470°C signifies a significant energy release phase, likely due to the combustion of the initial organic layers or phytochemicals associated with the nanoparticles. This peak occurs at a higher temperature than the initial exothermic peaks of rubber leaf nanoparticles, suggesting the presence of more thermally stable organic compounds in the oil palm leaf-derived nanoparticles [30]. The subsequent peak at 560°C indicates an additional phase of energy release, likely due to the breakdown of more complex and stable organic components. The fewer exothermic peaks compared to rubber leaf nanoparticles suggest a more simplified degradation process.

MgO nanoparticles derived from Awolowo leaves show exothermic peaks at 590°C and 660°C (Figure 3). These peaks indicate the energy release associated with the decomposition of highly stable organic molecules or phytochemicals. The exothermic peak at 590°C suggests the breakdown of organic components

that are more resistant to thermal degradation [31]. The higher temperature of this peak, compared to those observed in rubber and Oil Palm leaf nanoparticles, indicates that the organic materials associated with Awolowo leaf-derived MgO nanoparticles are more thermally stable. The subsequent peak at 660°C represents another stage of energy release, potentially due to the transformation of remaining organic materials or interactions between organic and inorganic components within the nanoparticles.

In summary, the TGA and DTA results provide distinct thermal degradation behaviors for MgO nanoparticles derived from different leaf sources. Rubber leaf-derived MgO nanoparticles show an initial low-temperature weight loss, followed by a significant mid-temperature loss, indicative of the presence of both volatile and stable organic components [32]. In contrast, Oil Palm leaf nanoparticles exhibit a pronounced initial weight loss, suggesting a larger quantity of volatile components, followed by a secondary loss of more stable organics. Awolowo leaf-derived MgO nanoparticles differ by undergoing a single, prolonged degradation phase, resulting in a higher residual content of stable inorganic MgO.

Furthermore, the exothermic peaks observed in these nanoparticles indicate variations in their thermal behaviors and energy release patterns. Rubber leaf MgO nanoparticles exhibit multiple exothermic peaks at lower temperatures (240°C, 360°C, and 600°C), indicating the presence of various stages of energy release associated with the degradation of both volatile and stable organic components [32, 33]. Oil Palm leaf nanoparticles, with exothermic peaks at 470°C and 560°C, suggest the presence of more thermally stable organic compounds, resulting in a more simplified degradation process compared to rubber leaf nanoparticles. Awolowo leaf-derived MgO nanoparticles, showing exothermic peaks at 590°C and 660°C, reflect the highest thermal stability, indicating the presence of highly stable organic materials [33, 34]. These variations in exothermic peaks emphasize the influence of the source plant's biochemical composition on the thermal and energy release characteristics of the synthesized nanoparticles. Understanding these differences is essential for tailoring the properties of MgO nanoparticles for specific applications, particularly those requiring precise thermal management and stability, such as photocatalytic studies [34, 35].

4.0 CONCLUSION

The comparative TGA/DTA analysis of bio-synthesized magnesium oxide (MgO) nanoparticles derived from Rubber (*Hevea brasiliensis*), Awolowo (*Chromolaena odorata*), and Oil Palm (*Elaeis guineensis*) leaves offers valuable insights into their thermal stability and degradation characteristics. The TGA profiles of these nanoparticles revealed distinct thermal degradation behaviours, reflecting the specific

phytochemical compositions from each plant source. These findings underscore the significance of selecting appropriate plant sources based on their phytochemical composition to optimize the thermal properties of MgO nanoparticles. This study not only contributes to the development of sustainable nanomaterial synthesis but also demonstrates the potential of utilizing tropical foliage extracts to produce MgO nanoparticles with tailored thermal characteristics. The insights from this research provide a foundation for future applications of bio-synthesized nanoparticles in diverse fields such as catalysis, materials science, and environmental remediation, where controlled thermal behaviour is paramount.

Acknowledgements:

We extend our heartfelt gratitude to all the technologists in the Department of Chemistry at the University of Benin and Ambrose Alli University for their invaluable support in ensuring the success of this analysis. Your contributions are deeply appreciated.

REFERENCES

- [1] McNamara, K., & Tofail, S. (2017). Nanoparticles in biomedical applications. *Advances in Physics: X*, 2(1), 54–88. <https://doi.org/10.1080/23746149.2016.1254570>
- [2] Gao, X., Du, C., Zhuang, Z., & Chen, W. (2016). Carbon quantum dot-based nanoprobe for metal ion detection. *Journal of Materials Chemistry C*, 4(31), 6927–6945. <https://doi.org/10.1039/C6TC02055K>
- [3] Farani, R., Farsadrooh, M., Zare, I., Gholami, A., & Akhavan, O. (2023). Green synthesis of magnesium oxide nanoparticles and nanocomposites for photocatalytic antimicrobial, antibiofilm and antifungal applications. *Catalysts*, 13(4). <https://doi.org/10.3390/catal13040642>
- [4] Klebowski, B., Depciuch, J., Parlińska-Wojtan, M., & Baran, J. (2018). Applications of noble metal-based nanoparticles in medicine. *International Journal of Molecular Sciences*, 19(12). <https://doi.org/10.3390/ijms19124031>
- [5] Essien, E., Atasie, V., Oyebanji, T., & Nwude, D. (2020). Biomimetic synthesis of magnesium oxide nanoparticles using *Chromolaena odorata* (L.) leaf extract. *Chemical Papers*, 74(7), 2101–2109. <https://doi.org/10.1007/s11696-020-01056-x>
- [6] Kongsawadworakul, P., Viboonjun, U., Romruensukharom, P., Chantuma, P., Ruderman, S., & Chrestin, H. (2009). The leaf, inner bark and latex cyanide potential of *Hevea brasiliensis*: Evidence for involvement of cyanogenic glucosides in rubber yield. *Phytochemistry*, 70(6), 730–739. <https://doi.org/10.1016/j.phytochem.2009.03.020>
- [7] Das, B., Moumita, S., Ghosh, S., Khan, I., Indira, D., Jayabalan, R., Tripathy, S., Mishra, A., & Balasubramanian, P. (2018). Biosynthesis of magnesium oxide (MgO) nanoflakes by using leaf extract of *Bauhinia purpurea* and evaluation of its antibacterial property against *Staphylococcus aureus*. *Materials Science & Engineering: C, Materials for Biological Applications*, 91, 436–444. <https://doi.org/10.1016/j.msec.2018.05.059>
- [8] Essien, E., Atasie, V., Nwude, D., Adekolurejo, E., & Owofe, F. (2022). Characterisation of ZnO nanoparticles prepared using aqueous leaf extracts of *Chromolaena odorata* (L.) and *Manihot esculenta* (Crantz). *South African Journal of Science*. <https://doi.org/10.17159/sajs.2022/11225>
- [9] Buniyamin, I., Asli, N., Eswar, K., Kadir, S., Saiman, A., Idorus, M., Mahmood, M., & Khusaimi, Z. (2024). Biosynthesis of Tin(IV) oxide nanoparticles (SnO₂ NPs) via *Chromolaena odorata* leaves: The influence of heat on the extraction procedure. *Journal of Science and Mathematics Letters*, 12(2). <https://doi.org/10.37134/jsml.vol12.2.11.2024>
- [10] Tow, W., Goh, A., Sundralingam, U., Palanisamy, U., & Sivasothy, Y. (2021). Flavonoid composition and pharmacological properties of *Elaeis guineensis* Jacq. leaf extracts: A systematic review. *Pharmaceuticals*, 14(10). <https://doi.org/10.3390/ph14100961>
- [11] Salem, S., & Fouda, A. (2020). Green synthesis of metallic nanoparticles and their prospective biotechnological applications: An overview. *Biological Trace Element Research*, 199(1), 344–370. <https://doi.org/10.1007/s12011-020-02138-3>
- [12] Abdullaeva, Z. (2017). Characterization of nanoparticles after biological synthesis. In *Nanotechnology and Biosensors* (pp. 177–195). https://doi.org/10.1007/978-3-319-54075-7_8
- [13] Khrantsov, P., Kalashnikova, T., Bochkova, M., Kropaneva, M., Timganova, V., Zamorina, S., & Rayev, M. (2020). Measuring the concentration of protein nanoparticles synthesized by desolvation method: Comparison of Bradford assay, BCA assay, hydrolysis/UV spectroscopy, and gravimetric analysis. *International Journal of Pharmaceutics*. <https://doi.org/10.26434/chemrxiv.13285712.v1>
- [14] Sharma, N., Vishwakarma, J., Rai, S., Alomar, T., AlMasoud, N., & Bhattarai, A. (2022). Green route synthesis and characterization techniques of silver nanoparticles and their biological adeptness. *ACS Omega*, 7(31), 27004–27020. <https://doi.org/10.1021/acsomega.2c01400>
- [15] Mullis, A., Jacobson, S., & Narasimhan, B. (2020). High-throughput synthesis and screening of rapidly-degrading polyanhydride nanoparticles. *ACS Combinatorial Science*. <https://doi.org/10.1021/acscombsci.9b00162>
- [16] Hurley, K., Ring, H., Kang, H., Klein, N., & Haynes, C. (2015). Characterization of magnetic nanoparticles in biological matrices.

- Analytical Chemistry*, 87(23), 11611–11619. <https://doi.org/10.1021/acs.analchem.5b02229>
- [17] Pedrosa, T., Estupiñán-López, C., & De Araujo, R. (2020). Temperature evaluation of colloidal nanoparticles by the thermal lens technique. *Optics Express*, 28(21), 31457–31467. <https://doi.org/10.1364/OE.405172>
- [18] Pielichowska, K., & Nowicka, K. (2019). Analysis of nanomaterials and nanocomposites by thermoanalytical methods. *Thermochimica Acta*. <https://doi.org/10.1016/j.TCA.2019.03.014>
- [19] Bharucha, S., Dave, M., Chaki, S., & Limbani, T. (2024). Thermal investigation of NbSe₂ nanoparticles synthesized through a temperature-dependent sonochemical method. *RSC Advances*, 14(50), 33459–33470. <https://doi.org/10.1039/d4ra05108d>
- [20] Kottala, R., Chigilipalli, B., Mukuloth, S., Shanmugam, R., Kantumuchu, V., Ainapurapu, S., & Cheepu, M. (2023). Thermal degradation studies and machine learning modelling of nano-enhanced sugar alcohol-based phase change materials for medium temperature applications. *Energies*, 16(5), 2187. <https://doi.org/10.3390/en16052187>
- [21] Ikhuoria, E. U., Uwidia, I. E., Otabor, G. O., & Ifijen, I. H. (2023). Comparative analysis of magnesium oxide nanoparticles biosynthesized from rubber seed shell and rubber leaf extracts. In *Biomedical Materials & Devices*. <https://doi.org/10.1007/s44174-023-00139-z>
- [22] Essien, E., Atasié, V., Oyebanji, T., & Nwude, D. (2020). Biomimetic synthesis of magnesium oxide nanoparticles using *Chromolaena odorata* (L.) leaf extract. *Chemical Papers*, 74(7), 2101–2109. <https://doi.org/10.1007/s11696-020-01056-x>
- [23] Venkatachalam, A., Jesuraj, J. P., & Sivaperuman, K. (2021). *Moringa oleifera* leaf extract-mediated green synthesis of nanostructured alkaline earth oxide (MgO) and its physicochemical properties. *Journal of Chemistry*, 2021, Article ID 4301504, 22 pages. <https://doi.org/10.1155/2021/4301504>
- [24] Mrig, S., Jennings, M., Bhide, M., Bakewell, C., & Knapp, C. (2022). Deposition of metallic silver from versatile amidinate precursors for use in functional materials. *Journal of Chemical Research*, 46. <https://doi.org/10.1177/17475198221075301>
- [25] Bharucha, S., Dave, M., Chaki, S., & Limbani, T. (2024). Thermal investigation of NbSe₂ nanoparticles synthesized through a temperature-dependent sonochemical method. *RSC Advances*, 14(50), 33459–33470. <https://doi.org/10.1039/d4ra05108d>
- [26] Essien, E., Atasié, V., Oyebanji, T., & Nwude, D. (2020). Biomimetic synthesis of magnesium oxide nanoparticles using *Chromolaena odorata* (L.) leaf extract. *Chemical Papers*, 74(7), 2101–2109. <https://doi.org/10.1007/s11696-020-01056-x>
- [27] Proniewicz, E., Vijayan, A., Surma, O., Szkudlarek, A., & Molenda, M. (2024). Plant-assisted green synthesis of MgO nanoparticles as a sustainable material for bone regeneration: Spectroscopic properties. *International Journal of Molecular Sciences*, 25(8), Article 84242. <https://doi.org/10.3390/ijms25084242>
- [28] Proniewicz, E., Vijayan, A., Surma, O., Szkudlarek, A., & Molenda, M. (2024). Plant-assisted green synthesis of MgO nanoparticles as a sustainable material for bone regeneration: Spectroscopic properties. *International Journal of Molecular Sciences*, 25(8), Article 84242. <https://doi.org/10.3390/ijms25084242>
- [29] Mohapatra, P., Behera, S., Sahoo, S., Mishra, A., Dalpati, A., Shubhadarshinee, L., Jali, B., Mohapatra, P., & Barick, A. (2024). Explore the effect of magnesium oxide nanoparticles decorated graphene oxide hybrid nanofillers reinforced polyaniline ternary nanocomposites on optical, thermal, and dielectric properties. *Advances in Natural Sciences: Nanoscience and Nanotechnology*. <https://doi.org/10.1088/2043-6262/ad7c1e>
- [30] Xiang, S., Lidong, F., Bian, X., Li, G., & Chen, X. (2020). Evaluation of PLA content in PLA/PBAT blends using TGA. *Polymer Testing*, 81, 106211. <https://doi.org/10.1016/j.polymertesting.2019.106211>
- [31] Pugazhendhi, A., Prabhu, R., Muruganantham, K., Shanmuganathan, R., & Natarajan, S. (2019). Anticancer, antimicrobial, and photocatalytic activities of green synthesized magnesium oxide nanoparticles (MgONPs) using aqueous extract of *Sargassum wightii*. *Journal of Photochemistry and Photobiology B: Biology*, 190, 86–97. <https://doi.org/10.1016/j.jphotobiol.2018.11.014>
- [32] Oladipo, A., Adeleye, O., Oladipo, A., & Aleshinloye, A. (2017). Bio-derived MgO nanopowders for BOD and COD reduction from tannery wastewater. *Journal of Water Process Engineering*, 16, 142–148. <https://doi.org/10.1016/j.jwpe.2017.01.003>
- [33] Matsukevich, I., Lipai, Y., & Romanovski, V. (2020). Cu/MgO and Ni/MgO composite nanoparticles for fast, high-efficiency adsorption of aqueous lead(II) and chromium(III) ions. *Journal of Materials Science*, 56(7), 5031–5040. <https://doi.org/10.1007/s10853-020-05593-4>
- [34] Nassar, M., Mohamed, T., Ahmed, I., & Samir, I. (2017). MgO nanostructure via a sol-gel combustion synthesis method using different fuels: An efficient nano-adsorbent for the removal of some anionic textile dyes. *Journal of Molecular Liquids*, 225, 730–740. <https://doi.org/10.1016/j.molliq.2016.10.135>
- [35] Demirci, S., Yildirim, B., Tünçay, M., Kaya, N., & Güllüoğlu, A. (2021). Synthesis,

characterization, thermal, and antibacterial activity studies on MgO powders. *Journal of*

Sol-Gel Science and Technology, 99(3), 576–588

